On the crystallinity of cellulose in wood: The newest findings lend further support to its non-crystalline nature

Umesh P. Agarwal,[1*] Richard S. Reiner,[1] Carlos Baez[2], Sally A. Ralph[1]

[1] Fiber and Chemical Sciences Research, USDA FS, Forest Products Laboratory, 1 Gifford Pinchot Drive Madison, WI 53726-2398.
[2] Analytical Chemistry and Microscopy Laboratory, USDA FS, Forest Products Laboratory, 1 Gifford Pinchot Drive Madison, WI 53726-2398.

ABSTRACT

The native state of wood-cellulose has proven to be difficult to explore. Contrary to the traditional acceptance of wood-cellulose being crystalline, in 2016, the authors' research reported that the cellulose was not crystalline.[1] New evidence, presented here, further supports the non-crystalline model. This evidence consisted of 64% H_2SO_4 hydrolysis of tension- and opposite-aspen woods (TW and OW, respectively), anatomical examination of the TW- and OW-woods, presence and absence of the 93 cm^{-1} Raman band, respectively, in TW G-layer and TW S_2 layer, and Raman spectra of TW-CNCs, wood holopulps, as well as those of mixture-samples of crystalline cellulose and xylan. Overall, these findings support the argument that the native wood-cellulose is non-crystalline.

KEYWORDS

Cell wall, CNCs, G-layer, Raman spectroscopy, XRD.

INTRODUCTION

Green wood contains water in addition to cellulose, lignin, and hemicelluloses. Water has unique influence not only on the properties of green wood but also on the structures of cellulose and hemicelluloses.[2, 3] Nevertheless, water's role in living plant cell walls and how it interacts with cell wall polysaccharide components remains not well understood.[3] Moreover, even before water-cellulose interactions can be elucidated, the understanding of cellulose's structure remains complicated. Traditionally, wood cellulose has been considered as a crystalline material, [4 - 7] and it has been reported that simulated XRD patterns based on the crystallite size of cellulose can alone explain the diffraction pattern of cellulose materials.[7 - 9] Recent research has pointed to a situation where the existing model of wood cellulose as being crystalline is no longer valid and instead, a non-crystalline model is likely. [1, 10] This conclusion was based on the following findings: a) wood-cellulose in the never-dried native state is laterally aggregated where internal chains are water-accessible, b) hydroxymethyl groups (CH_2OH) in cellulose exist not only in the *tg* conformation but also in the *gt* rotamer form, c) in native-state fibrils, low-frequency Raman bands due to cellulose crystal domains are absent, indicating the lack of crystallinity, d) failure of the normal 64 % H_2SO_4 hydrolysis procedure to produce cellulose nanocrystals from untreated wood, and e) deuterated-CNCs could be generated from the hydrothermally treated poplar indicating that cellulose chains were accessible to water and thereby became partly crystalline upon the hydrothermal treatment.[10] Moreover, it was reported that with higher treatment temperature, more crystalline cellulose was produced. If wood-cellulose was already crystalline, that cannot happen. In the context of the present work, the crystalline cellulose is defined as a structure that has a crystal lattice that extends in all directions (translational periodicity) and therefore, having long-range positional order. Moreover, water and most other small molecules cannot get into the crystalline cellulose. Additionally, the work of some other researchers based on six primary grass and Arabidopsis cell walls is also relevant where they showed that in the interior of plant primary cell wall microfibrils cellulose has five different conformations and that cellulose ^{13}C NMR chemical shifts differed significantly from the 13C chemical shifts of the Iα and Iβ allomorphs.[11] And therefore, in the opinion of the authors, such cell wall cellulose cannot be crystalline because, within the fibril, the cellulose conformations and the resulting H-bonding patterns between the chains would be different.[11, 12] The existence of the above-mentioned different cellulose conformations in the primary wall further supported the results of an earlier study where the primary cell wall microfibrils of celery collenchyma contained extensive disorder in lateral packing, conformation, and hydrogen bonding.[13] Even though these microfibrils extensive disorder, their XRD resembled that of crystalline cellulose.[13] This further supported the conclusion that non-crystalline cellulose can contribute in the same XRD region as crystalline cellulose. The understanding of wood-cellulose supramolecular structure is important to numerous fields. For instance, areas such as cellulose biosynthesis, plant growth and function, biorefinery, cellulose nanomaterials, and wood science and technology, in general, would all benefit.

EXPERIMENTAL

All chemicals, reagents, celluloses, and holopulps and CNCs were obtained as reported recently by Agarwal et al. [14] This publication also describes how the following analyses/investigations were carried out - AFM imaging, compositional analysis of the samples, anatomical observations of woods, investigation of TW-wood cell walls by confocal Raman microscopy, analyses of various materials by FT-Raman and estimation of cellulose-crystallinity by this technique, and lastly, analysis by X-ray diffraction and estimation of cellulose crystallinity by Segal-WAXS method.

RESULTS AND DISCUSSION

Crystalline nature of G-layer:

Although it is widely reported that G-layer in TW is made up of crystalline cellulose, based on confocal Raman spectra (Fig. 1), where spectra of pure G-layer, pure S_2, and MCC (highly crystalline cellulose) are compared, this conclusion was further corroborated.

Here, it can be noted that, in the spectrum of S_2, a peak of cellulose at 93 cm^{-1} is absent while the contribution of lignin at 1600 cm^{-1} is present. Because the 93 cm^{-1} feature is an aspect of crystalline cellulose, this suggested that S_2 cellulose is unlikely to be crystalline. Moreover, the spectra of G-layer and MCC (Segal CrI 89.7%) were very similar (Fig. 1), and both contained the peak at 93 cm^{-1}, indicating that the former was composed of highly crystalline cellulose.[10] Previously, the contributions at 93, 172, and 380 cm^{-1} have been reported to be due to cellulose crystals. [10, 15] Additionally, it has been reported that the 93 cm^{-1} band, assigned to rotation of cellulose molecule, [16] is capable of distinguishing between the crystalline and organized (but not-crystalline) phases of cellulose. [10] This low energy band of crystalline cellulose has also been detected by another type of spectroscopy, terahertz spectroscopy,[17, 18] where lattice modes of organic molecules and polymers are usually detected.[19, 20] 93 cm^{-1} wavenumber corresponds to 2.8 THz and is detected in that region in terahertz spectroscopy. In any case, the aspect that G-layer is composed of almost pure crystalline cellulose, is extensively documented.[21 - 24] This is also supported by the spectra in Fig. 1 where the Raman spectra of S_2, G-layer, and MCC in 70-1700 cm^{-1} region are compared. It needs to be noted that in the S_2 spectrum, in addition to the contributions of cellulose, contributions of aspen lignin are present at 1661, 1595, 1455, 1331, 1130, 1037, 598, 531, and 369 cm^{-1} which were not detected in the spectra of the cotton and G-layer. [25, 26] In this spectrum (Fig. 1), the syringyl-lignin contribution at 369 cm^{-1} makes the 380 cm^{-1} cellulose peak broader on the low frequency side compared to the widths of this peak in the G-layer and MCC spectra.

Production of CNCs:

The yields of the CNCs obtained from similar amounts of TW- and OW-holopulps are listed in Table 1. In all probability, TW-CNCs (yield 20.7 %, Table 1) came from the G-layer because normal cell wall cellulose in known to produce no CNCs (Agarwal et al. 2016). Compared to the TW-holopulp, the amount of CNCs produced by the OW-holopulp (5.4%, Table 1) was 74% lower. Moreover, chemical composition analysis (Table 2) indicated that compared to the TW-holopulp the amount of glucan in the OW-holopulp was 20% lower. Accordingly, accounting for this difference, the yield from the opposite wood (or holopulp) should have been 16.6%, instead of 5.4% (Table 1). However, this assumes no difference in the capability of the two types of cell wall celluloses to produce CNCs. Nevertheless, considering the fact that CNCs can only be produced from crystalline cellulose (and therefore, G-layer) but not from the other wood cell walls and that the OW-holopulp (or OW) is not supposed to have any G-layer according to the literature,[27 - 29] production of the CNCs from OW-holopulp was not expected. Therefore, how does one explain the generation of the OW-CNCs? To answer this question, an anatomical analysis of the TW and OW was carried out (see below). The investigation revealed that G-layer existed in the OW, albeit sparingly, accounting for the low amount of CNCs production from this wood.

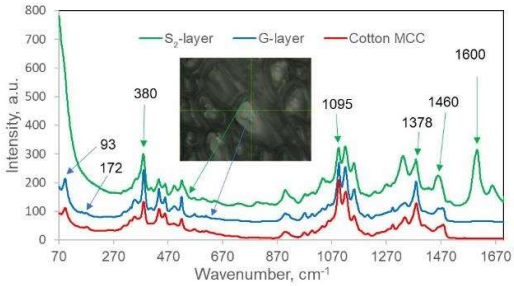

Figure 1. Comparison of 70–1700 cm^{-1} Raman spectra of pure G-layer with pure S_2 and MCC (highly crystalline cellulose, Segal CrI = 89.7%,[30]) (the inset shows the TW regions – G-layer and S_2, from which the shown spectra were obtained).

Table 1. CNCs: yield and analysis data

Sample	Yield, %	Mean height, nm	Crystallinity, %
			Segal-XRD;93-Raman; 380-Raman
TW-CNCs	20.7[a]	4.0 ± 1.6	95.5; 69.7; 80.2
OW-CNCs	5.4[a]	3.1 ± 1.4	93.5; 59.2; 73.7
Pulp-CNCs	50.0[b]	4.3 ± 1.4	86.0; 46.4[c]; 55.5[c]

[a]Based on wood holopulp; [b]Based on softwood bleached kra pulp; [c]Data from [31].

Anatomical analysis:

Images of the TW and OW cross-sections that were counterstained with 1:1 aqueous safranin O and Alcian Blue are shown in Fig. 2(A) and Fig. 2(B). In Fig. 2(A), fibers with prominent, thick G-layers (clearly staining blue) represent well over 99% of all fibers; very few fibers without a G -layer over many square millimeters of tissue were observed. On the other hand, surprisingly, OW fibers with G-layers (clearly staining blue) were found although sparsely – less than ~10% of observed fibers. G-layers were typically thin, and the gelatinous fibers were distributed diffusely throughout the growth ring. Vessel-adjacent cells

sometimes showed some blue-staining cell contents which was not consistent with a separated G layer.

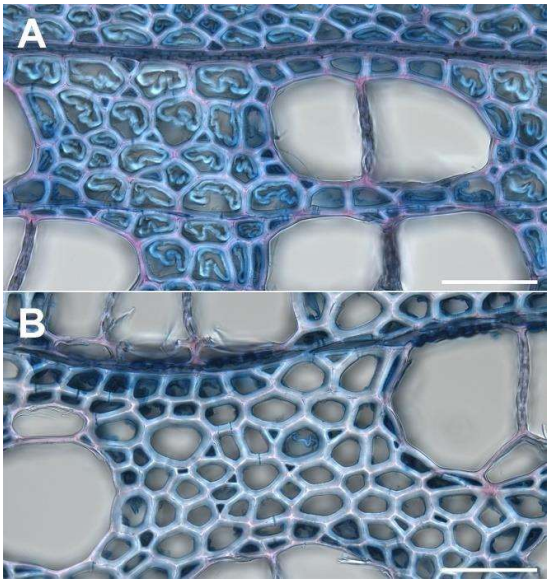

Figure 2. Transmitted light micrographs of stained transverse sections of aspen. (A) Tension wood (TW) showing conspicuous gelatinous layers in the great majority of the fibers. (B) Opposite wood (OW) showing a fiber with a gelatinous layer; Scale bars 200 µm

Raman spectra:

The intent was to find out how the Raman spectra of various holopulps (TW-, OW-, and aspen, Table 2) compare with each other and also with a set of samples prepared by mixing specific amounts of cotton MCC (WhatmanCC31, highly crystalline cellulose) and xylan. The results would further help address the question of the presence of crystalline cellulose in normal cell walls of woody tissue. Nine mixture samples of the following MCC:xylan compositional ratios were made – 90:10, 80:20, 70:30, 60:40, 50:50, 40:60, 30:70, 20:80, and 10:90. The purpose was to not only cover the range of possible hemicellulose and Klason lignin contents in the wood holopulp samples (which in the mixtures is represented by xylan, Table 2), but also to see at what low concentration of cellulose, in the mixture samples, the crystalline-cellulose peaks at 93 and 172 cm^{-1} can no longer be detected. Moreover, could these two bands be detected in the Raman spectra of various holopulps at the glucan:xylan concentrations listed in Table 2. To simplify this, to a first approximation, the holopulps are assumed to be solely made up of cellulose and xylan (i.e., the amounts of xylan, mannan, arabinan, galactan, and Klason lignin were added and counted as xylan, Table 2). This is justifiable considering the fact that, for most of the samples, xylan is the dominant component of the non-glucan constituents and mannan occurs in much smaller amount (Table 2). In case the Raman bands could be detected in the mixture (having similar glucan:xylan composition as in the holopulp) but not in the corresponding holopulp, then it would imply that the cellulose in the holopulp was not as crystalline as the MCC. On the other hand, if the bands were to be detected in both the samples (mixture and the corresponding holopulp), it would imply that the holopulp-cellulose was as crystalline as the MCC.

Table 2: Chemical composition (%)

Sample	Klason lignin	Glucan	Xylan	(Man. + Arab. + Gal.)	Ratio, Glucan :xylan[e]
TW	18.3	46.9	13.5	1.7	NA[a]
OW	22.2	42.0	15.5	3.2	NA
TW holopulp	1.6	61.3	15.2	0.2	78:22
OW holopulp	2.80	49.0	17.5	3.1	68:32
Aspen holopulp[c]	3.1	52.3	16.7	1.7	71:39
SWBKP	0.5	81.3	7.5	5.5	86:14
Cotton MCC[d]	3.1	92.2	0.1	ND[b]	97:3

[a]Not applicable; [b]Not detected; [c]Reference [32]; [d]Reference [33]; [e]the amounts of xylan, mannan (man.), arabinan (arab.), galactan (gal.), and Klason lignin were added and counted as xylan (see text).

In Fig. 3A, low-frequency (70 – 550 cm^{-1}) spectra of the holopulps are compared with the spectra of TW-CNCs and SWBKP. Among the holopulps, the spectral peaks at 93 and 172 cm^{-1} were detected, albeit as shoulders, for only TW-holopulp. Moreover, in the spectra of the remaining holopulps, OW-holopulp's contribution at 172 cm^{-1} was hardly noticeable and not perceptible at all at 93 cm^{-1} whereas for the aspen holopulp, none of these bands were noticeable (Fig. 3A). In the case of TW-holopulp, the appearance of the features can be explained by the fact that it contained significant amount of crystalline cellulose (G-layer). On the other hand, a much-reduced amount of this layer was present in the OW-holopulp and therefore, the contribution of crystalline cellulose was not evident. Absence of the twin features at 93 and 172 cm^{-1} in the spectra of aspen holopulp argues for the absence of any crystalline cellulose because not only G-layer was absent, but also the cell wall cellulose was not crystalline, as was previously reported. [1, 10]

Considering the spectra of the MCC:xylan mixtures (Fig. 3B), it is clear that peaks at 93 and 172 cm^{-1} are detectable, respectively, up to the MCC:xylan compositional ratios of 40:60 and 60:40. This difference in the detectability of the two bands has to do with the fact that the band at 172 cm^{-1} is much

weaker compared to the 93 cm^{-1} band (Fig. 3A, TW CNC spectrum). In any case, had the cell wall cellulose been highly crystalline in normal cell walls, the holopulp where the glucan:xylan compositional ratio is 71:39 (Table 2), both the bands should have been seen (Fig. 3A and Fig. 3B, Table 2). That not being the case, as demonstrated in Fig. 3C, the spectra provide evidence in support for the cellulose being not highly crystalline.

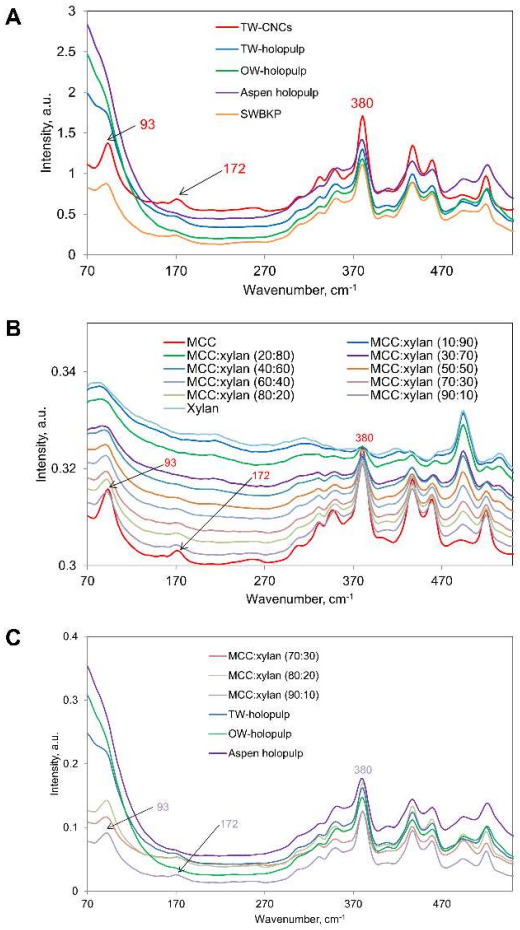

Figure 3. (A) Raman spectra of three holopulps, SWBKP, and TW-CNCs, (B) Raman spectra of mixtures of MCC:xylan at various compositions, (C) Comparing the spectra of various holopulps and the appropriate MCC:xylan mixtures (70:30, 80:20, and 90:10). The annotated peaks in Fig. 3A, Fig. 3B, and Fig. 3C are, respectively, from TW-CNCs, MCC, and MCC:xylan (90:10).

X-ray diffraction:

XRDs of tunicin, aspen, amorphous cellulose, and TW-CNCs are shown in Fig. 4. Except for the CNCs the information is taken from the authors prior investigations. [10, 30, 32, 33] Due to its very high crystallinity, tunicin showed the sharpest and most resolved peaks. As expected, compared to tunicin's XRD (Fig. 4A), the diffractogram of TW-CNCs is less resolved, most likely due to the smaller size of its crystals in relation to that of tunicin's. But the diffractogram is still quite strong, as was expected based on the Raman spectrum of the G-layer (Fig. 1). However, important to note in Fig. 4A are the significantly weaker and broader characteristics of the diffraction pattern of wood where (1-10) and (110) peaks remained completely unresolved and (200) peak was rather broad. If indeed the wood-cellulose was crystalline, an XRD similar to that of TW-CNCs would have been obtained, which was clearly not the case. Moreover, between TW-CNCs and wood cellulose, the fibril/crystal size difference does not exist because both are approximately 3 nm wide (Table 1).[31, 34] And therefore, although the effect of cellulose crystal size on XRD has been reported in the literature,[8] when comparing the two XRDs (Fig. 4A), effect of fibril/crystal-size on the wood XRD does not apply. However, further considering that in cell walls ~ 15 nm wide cellulose microfibril bundles exist,[35] the increased bundle size compared to 3 nm wide fibrils is likely to produce narrower peaks in the XRD. This is likely due to the increased order at the interface of the combined fibrils where the cellulose chains have lower deformation flexibility. Moreover, microfibril shape is also not likely to be a factor because under this scenario,[7] fibrils are still crystalline and therefore, a 93 cm^{-1} peak in Raman spectroscopy should have been seen. Consequently, most likely, the width of the wood XRD originates from the fact that the cellulose is not crystalline. The difference between the XRDs of wood and amorphous cellulose is shown in Fig. 4B and clearly, in many regions of 2θ the contributions overlap, if not similar. Therefore, in the view of the authors, an aggregated phase of cellulose in wood that is non-crystalline but organized/aligned in some fashion, is likely to produce such a diffractogram. This hypothesis is supported by the fact that water induced reorganization of cellulose gives rise to increased contributions at 2θ positions where crystalline cellulose also contributes.[30, 33] Due to this organization, compared to amorphous cellulose, the long-range order increases and as seen in Fig. 6B, stronger contributions are likely to be generated in 2θ regions 14 - 17° and 21 – 24°. Additionally, based on to the classic Bragg scattering (Eq. 1), in a non-crystalline solid, as the distance between molecular scattering entities changes (d is variable as the interatomic distance changes in a sample) scattering angle θ and therefore, the positions of the intensity contributions also vary, thus giving rise to the broadness of the wood-cellulose XRD (Fig. 4B). Accordingly, the XRD data analysis further supported the non-crystalline nature of wood cellulose.

$$\lambda = 2d \sin\theta \qquad (1)$$

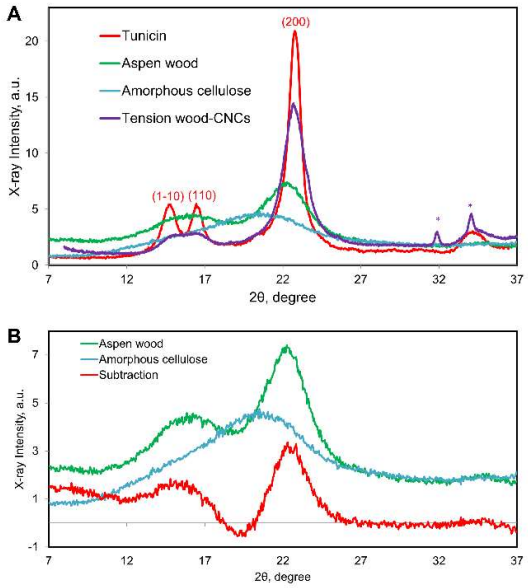

Figure 4. (A) Comparison of XRDs of amorphous cellulose, aspen wood, TW-CNCs, and tunicin; (B) Result of subtraction of the XRDs (aspen wood – amorphous cellulose). In (A) peaks marked with * are due to Na_2SO_4 impurity and the annotated peaks are of tunicin.

CONCLUSIONS

In this study, to understand the nature of wood cellulose in native state, further research using tension aspen wood was carried out. All of the obtained results supported the earlier reported finding that wood cellulose is not crystalline. Raman spectra obtained from distinct S_2 and G-layer regions of TW suggested that the spectrum of the former lacked a crystallinity-specific band at 93 cm^{-1} which was present in the G-layer. When the G-layer rich TW was hydrolyzed by 64% H_2SO_4, CNCs were obtained and therefore, obviously, such a treatment did not destroy the crystalline cellulose. On the other hand, the yield of the CNCs from the opposite wood was very low due to the fact that such wood contained very little G-layer. The acid hydrolysis data obtained here clearly supported the earlier finding that when untreated softwood is hydrolyzed by the 64% H_2SO_4, no CNCs were produced. Other analysis that consisted of comparing the Raman spectra of various wood-holopulps with those of the mixtures of crystalline-cellulose and xylan at compositions representative of the holopulps indicated that except in the case of TW-holopulp, the spectra of the holopulps lacked the crystalline cellulose features at 93 and 172 cm^{-1}. Similarly, the XRD analysis of four materials - amorphous cellulose, aspen wood, TW-CNCs, and tunicin, provided further support to the view that, in the native state, cell wall cellulose is non-crystalline.

ACKNOWLEDGEMENTS

The authors are very thankful to Alex Wiedenhoeft (Wood Anatomy and Forest Mycology Group, FPL) for carrying out the anatomical analysis of the wood samples. The authors gratefully acknowledge the use of X-ray facilities and instrumentation supported by NSF through the University of Wisconsin Materials Research Science and Engineering Center (DMR-1121288).

REFERENCES

[1] Agarwal, U.P., Ralph, S.A., Reiner, R.S., and Baez, C. (2016). Probing crystallinity of never-dried wood cellulose with Raman spectroscopy. Cellulose 23: 125–144. DOI: 10.1007/s10570-015-0788-7.

[2] Cresswell, R., Dupree, R., Brown, S.P., Pereira, C.S., Skaf, M.S., Sorieul, M., Dupree, P., and Hill, S. (2021). Importance of water in maintaining softwood secondary cell wall nanostructure. Biomacromolecules 22: 4669–4680, DOI: 10.1021/acs.biomac.1c00937.

[3] Penttila, P.A., Altgen, M., Carl, N., van der Linden, P., Morfin, I., Osterberg, M., Schweins, R., and Rautkari, L. (2020). Moisture-related changes in the nanostructure of woods studied with X-ray and neutron scattering. Cellulose 27: 71–87, DOI: 10.1007/s10570-019-02781-7.

[4] Andersson, S., Serimaa, R., Paakkari, T., Saranpaa, P., and Pesonen, E. (2003) Crystallinity of wood and the size of cellulose crystallites in Norway spruce (Picea abies). J. Wood Sci. 49: 531–537, DOI: 10.1007/s10086-003-0518-x.

[5] Leppanen K, Andersson S, Torkkeli M, Knaapila M, Kotelnikova N, Serimaa R (2009) Structure of cellulose and microcrystalline cellulose from various wood species, cotton and flax studied by X-ray scattering. Cellulose 16: 999–1015, DOI: 10.1007/s10570-009-9298-9.

[6] Fernandes, A.N., Thomas, L.H., Altaner, C.M., Callow, P., Forsyth V.T., Apperley, D.C. Kennedy, C.J., and Jarvis, M.C. (2011). Nanostructure of cellulose microfibrils in spruce wood. Proc. National Acad. Sci. 108: E1195–E1203, DOI: 10.1073/pnas.1108942108.

[7] Newman, R.H. Hill, S.J., Harris P.J. (2013). Wide-angle X-ray scattering and solid-state nuclear magnetic resonance data combined to test models for cellulose microfibrils in mung bean cell walls. Plant Physiol. 163:1558–156, DOI: 10.1104/pp.113.228262.

[8] French, A.D., and Cintron, M.S. (2013). Cellulose polymorphy, crystallite size, and the Segal crystallinity index. Cellulose 20: 20:583–588, DOI: 10.1007/s10570-012-9833-y.

[9] Nam, S., French, A.D., Condon, B.D., Concha, M. (2016). Segal crystallinity index revisited by the simulation of X-ray diffraction patterns of cotton cellulose Iβ and cellulose II. Carbo. Poly. 135: 1–9, DOI: 10.1016/j.carbpol.2015.08.035.

[10] Agarwal, U.P., Ralph, S.A., Reiner, R.S., and Baez, C. (2018). New cellulose crystallinity estimation method that differentiates between organized and crystalline phases. Carbohy. Poly. 190: 262–270, DOI: 10.1016/j.carbpol.2018.03.003.

[11] Wang, H., Tsuchikawa, S., and Inagaki, T. (2021). Terahertz time-domain spectroscopy as a novel tool for crystallographic analysis in cellulose: the potentiality of being a new standard for evaluating crystallinity. Cellulose 28: 5293–5304. DOI: 10.1007/s10570-021-03902-x.

[12] Jarvis, M.C. (2018). Structure of native cellulose microfibrils, the starting point for nanocellulose manufacture. Phil. Trans. Math. Phys. Eng. Sci. 376: 20170045, http://dx.doi.org/10.1098/rsta. 2017.0045.

[13] Thomas, L.H., Forsyth, V.T., Šturcová, A., Kennedy, C.J., May, R.P., Altaner, C.M., Apperley, D.C., Wess, T.J., and Jarvis, M.C. (2013). Structure of cellulose microfibrils

in primary cell walls from collenchyma. Plant Physiol 161: 465–476, DOI: 10.1104/pp.112.206359.
[14] Agarwal, U.P., Reiner, R.S., Baez, C., and Ralph, S.A., (2023). Native state of wood cellulose: evidence that further supports its non-crystalline nature. Holzforschung 77 (published online). DOI: 10.1515/hf-2022-0176.
[15] Agarwal, U.P. (2014). 1064 nm FT-Raman spectroscopy for investigations of plant cell walls and other biomass materials. Front. Plant Sci. 5:490, DOI: 10.3389/fpls.2014.00490.
[16] Makarem, M., Lee, C.M., Kafle, K., Huang, S., Chae, I., and Kim, S.H. (2019). Probing cellulose structures with vibrational spectroscopy. Cellulose 26: 35–79, DOI: 10.1007/s10570-018-2199-z.
[17] Vieira, F. S. and Pasquini, C. (2014). Determination of cellulose crystallinity by terahertz time domain spectroscopy. Anal. Chem. 86: 3780–3786. DOI: 10.1021/ac4035746.
[18] Wang, T., Yang, H., Kubicki, J.D., and Hong, M. (2016). Cellulose structural polymorphism in plant primary cell walls investigated by high-field 2D solid-state NMR spectroscopy and density functional theory calculations. Biomacromolecules 17: 2210–2222.
[19] Parrott, E.P.J. and Zeitler, J.A. (2015). Terahertz time-domain and low-frequency Raman spectroscopy of organic materials. Appl. Spectro. 69: 1–25, DOI: 10.1366/14-07707.
[20] Funaki, C., Toyouchi, T., Hoshina, H., Ozaki, Y., and Sato, H. (2017) Terahertz imaging of the distribution of crystallinity and crystalline orientation in a poly(e-caprolactone) film. Appl. Spectro. 71: 1537–1542, DOI: 10.1177/00037028166848.
[21] Dadswell, H.E. and Wardrop, A.B. (1955). The structure and properties of tension wood. Holzforschung 9: 97–103, DOI: 10.1515/hfsg.1955.9.4.97.
[22] Muller, M., Burghammer, M., and Sugiyama, J. (2006). Direct investigation of the structural properties of tension wood cellulose microfibrils using microbeam X-ray fiber diffraction. Holzforschung 60: 474–479, DOI: 10.1515/HF.2006.07.
[23] Pilate, G., Dejardin, A., Laurans, F., and Leple, J-C. (2004). Tension wood as a model for functional genomics of wood formation. New Phytol. 164: 63–72, DOI: 10.1111/j.1469-8137.2004.01176.x.
[24] Wada, M., Okano, T., Sugiyama, J., and Horii, F. (1995). Characterization of tension and normally lignified wood cellulose in Populus maximowiczii. Cellulose 2: 223–233. DOI: 10.1007/BF00811814.
[25] Agarwal, U.P. (2006). Raman imaging to investigate ultrastructure and composition of plant cell walls: Distribution of lignin and cellulose in black spruce wood (Picea mariana). Planta 224: 1141-1153, DOI: 10.1007/s00425-006-0295-z.
[26] Agarwal, U.P. McSweeny, J.D. and Ralph, S.A. (2011) FT–Raman investigation of milled-wood lignins: softwood, hardwood, and chemically modified black spruce lignins. J. Wood Chem. Technol. 31: 324–344, DOI: 10.1080/02773813.2011.562338.
[27] Coutand, C., Jeronimidis, G., Chanson, B., and Loup, C. (2004). Comparison of mechanical properties of tension and opposite wood in Populus. Wood Sci. Techno. 38: 11–24, DOI: 10.1007/s00226-003-0194-4.
[28] Gao, J., Jebrane, M., Terziev, N., and Daniel, G. (2021). Enzymatic hydrolysis of the gelatinous layer in tension wood of Salix varieties as a measure of accessible cellulose for biofuels. Biotechnol. Biofuels, 14: 141. DOI: 10.1186/s13068-021-01983-1.
[29] Mellerowicz, E.J., Immerzeel, P., and Hayashi, T. (2008). Xyloglucan: The molecular muscle of trees. Annals of Botany 102: 659–665, DOI: 10.1093/aob/mcn170.
[30] Agarwal, U.P., Ralph, S.A., Baez, C., and Reiner, R.S. (2021). Contributions of crystalline and noncrystalline cellulose can occur in the same spectral regions: Evidence based on Raman and IR and its implication for crystallinity measurements. Biomacromolecules 22: 1357–1373, DOI: 10.1021/acs.biomac.0c01389.
[31] Agarwal, U. P., Reiner, R.S., Ralph, S.A., Catchmark, J., Chi, K., Foster, E.J., Hunt, C. G., Baez, C., Ibach, R.E., and Hirth, K.C. (2021). Characterization of the supramolecular structures of cellulose nanocrystals of different origins. Cellulose 28: 1369–1385, DOI: 10.1007/s10570-020-03590-z.
[32] Agarwal, U.P., Reiner, R.S., and Ralph, S.A. (2013). Estimation of cellulose crystallinity of lignocelluloses using near-IR FT-Raman spectroscopy and comparison of the Raman and Segal-WAXS methods. J. Agric. Food Chem. 61: 103−113, DOI: 10.1021/jf304465k.
[33] Agarwal, U.P., Ralph, S.A., Baez, C., Reiner, R.S., and Verrill, S.P. (2017). Effect of sample moisture content on XRD-estimated cellulose crystallinity index and crystallite size. Cellulose 24: 1971–1924, DOI: 10.1007/s10570-017-1259-0.
[34] Saito, T., Kimura, S., Nishiyama, Y., and Isogai, A. (2007). Cellulose nanofibers prepared by TEMPO-mediated oxidation of native cellulose. Biomacromolecules 8: 2485-2491, DOI: 10.1021/bm0703970.
[35] Abe, K., Iwamoto, S., and Yano, H. (2007). Obtaining cellulose nanofibers with a uniform width of 15 nm from wood. Biomacromolecules 8: 3276-3278, DOI: 10.1021/bm700624p.